Electronic Supplementary Information

Regulating the electronic properties of $MoSe_2$ to improve its CO_2 electrocatalytic reduction performance via atomic doping

Jingjing Ye[a], Dewei Rao*[ab], and Xiaohong Yan*[a]

[a] *School of Materials Science and Engineering, Jiangsu University, Zhenjiang 212013, P. R. China.*
Fax: +86-511-88783268
Email: dewei@ujs.edu.cn; yanxh@ujs.edu.cn
[b] *Department of Chemistry and Biochemistry, University of California, 1156 High Street, Santa Cruz, CA 95064, United States.*

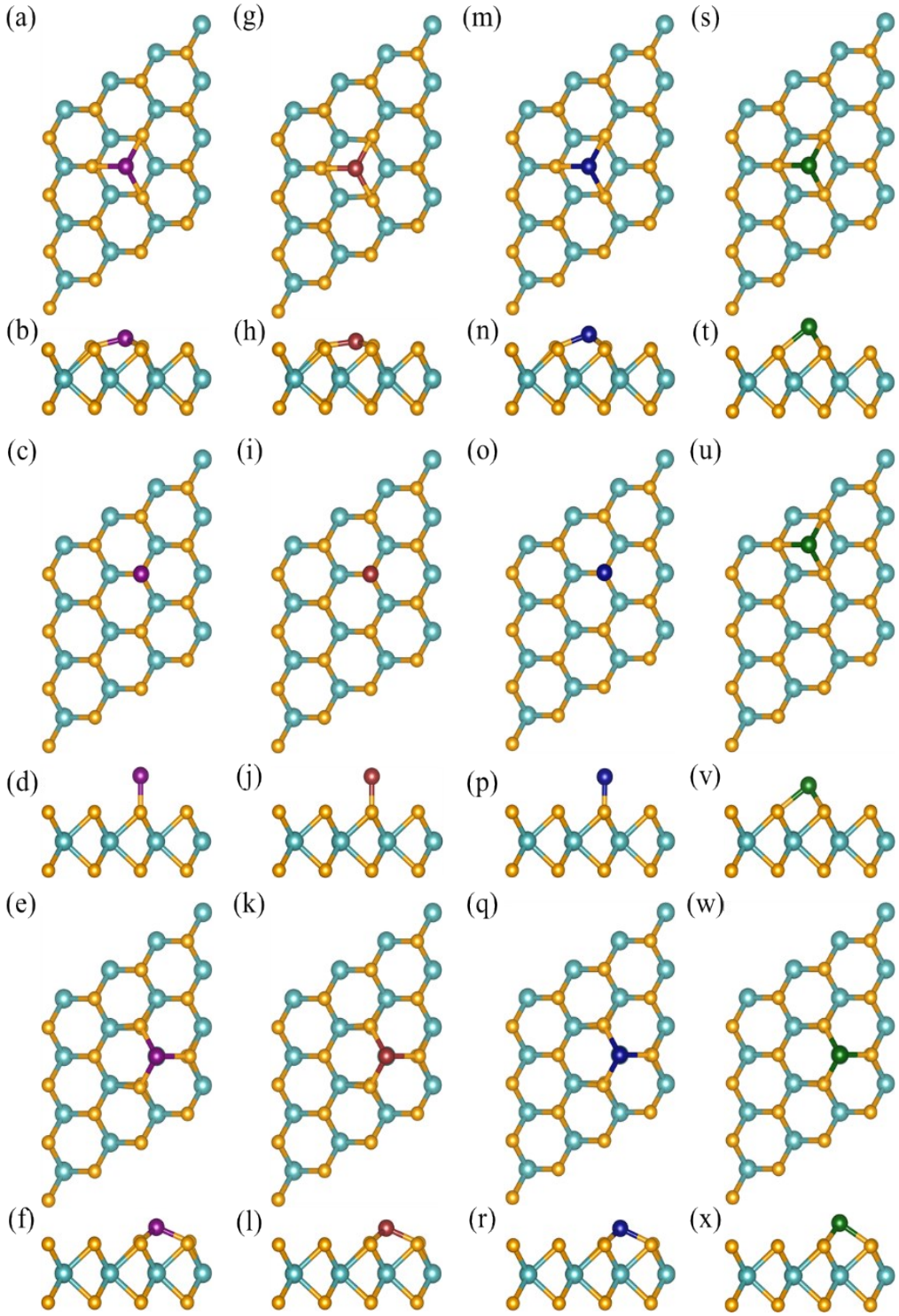

Fig. S1 Top and side views of the optimized structures of (a-b) $Fe_H@MoSe_2$, (c-d) $Fe_{ST}@MoSe_2$, (e-f) $Fe_{MT}@MoSe_2$, (g-h) $Co_H@MoSe_2$, (i-j) $Co_{ST}@MoSe_2$, (k-l) $Co_{MT}@MoSe_2$, (m-n) $Ni_H@MoSe_2$, (o-p) $Ni_{ST}@MoSe_2$, (q-r) $Ni_{MT}@MoSe_2$, (s-t) $Cu_H@MoSe_2$, (u-v) $Cu_{ST}@MoSe_2$ and (w-x) $Cu_{MT}@MoSe_2$ catalyst. The orange, blue, purple, brown, dark blue and green balls represent Se, Mo, Fe, Co, Ni and Cu atoms, respectively.

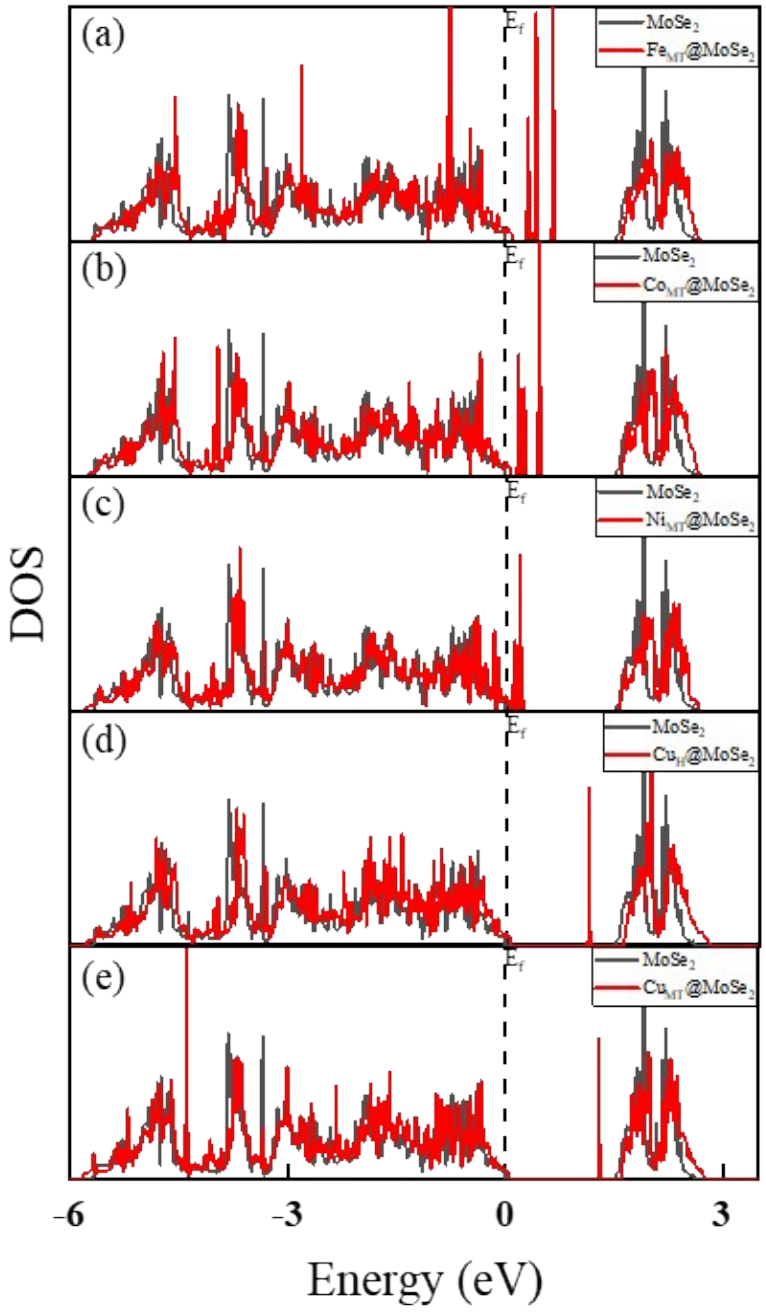

Fig. S2 Density of states (DOS) of (a) $Fe_{MT}@MoSe_2$, (b) $Co_{MT}@MoSe_2$, (c) $Ni_{MT}@MoSe_2$ (d) $Cu_H@MoSe_2$ and (e) $Cu_{MT}@MoSe_2$. The dotted line denotes the Fermi level, the red and grey lines represent the density of states of $TM@MoSe_2$ and $MoSe_2$, respectively.

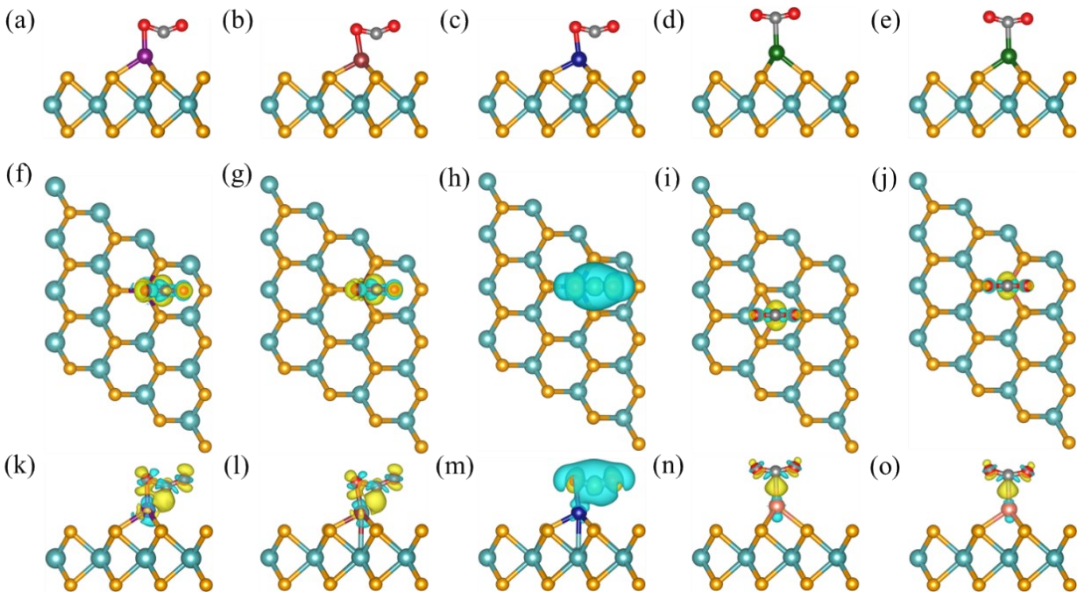

Fig. S3 Optimized structure of CO_2 adsorbed on (a) Fe_{MT}@$MoSe_2$, (b) Co_{MT}@$MoSe_2$, (c) Ni_{MT}@$MoSe_2$ (d) Cu_H@$MoSe_2$ and (e) Cu_{MT}@$MoSe_2$. (f-j) the top and (k-o) side views of isosurface of charge density difference of TM@$MoSe_2$. The yellow areas represent charge accumulation and the blue areas represent charge depletion. The value of isosurface is 0.0045 eV/Å^3. The orange, blue, purple, brown, dark blue, green, grey and red balls represent Se, Mo, Fe, Co, Ni, Cu, C and O atoms, respectively.

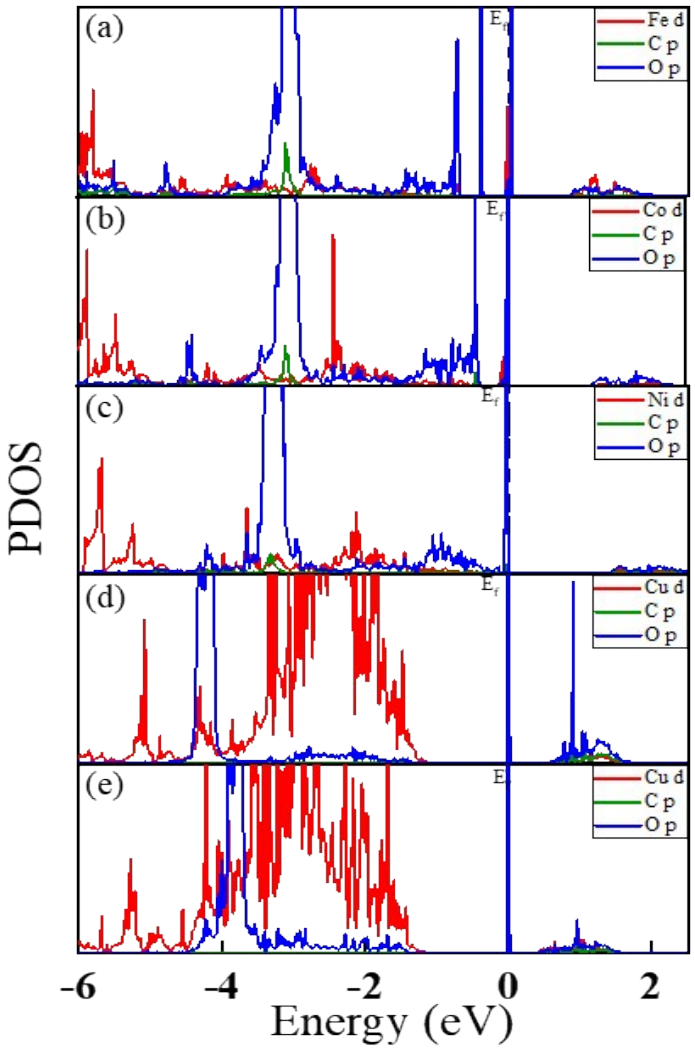

Fig. S4 Partial density of states (PDOS) of CO_2 adsorbed on (a) $Fe_{MT}@MoSe_2$, (b) $Co_{MT}@MoSe_2$, (c) $Ni_{MT}@MoSe_2$ (d) $Cu_H@MoSe_2$ and (e) $Cu_{MT}@MoSe_2$. The dotted line denotes the Fermi level (E_f), the red, green, and blue lines represent the 3d orbital of the metal atom, and the 2p orbital of the carbon or oxygen atom of CO_2, respectively.

	$Fe_{MT}@MoSe_2$	$Co_{MT}@MoSe_2$	$Ni_{MT}@MoSe_2$	$Cu_H@MoSe_2$	$Cu_{MT}@MoSe_2$
*COOH	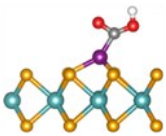	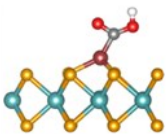	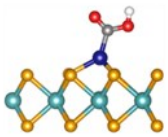	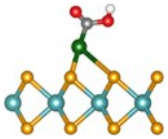	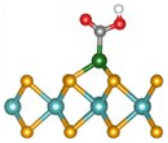
*COOH'	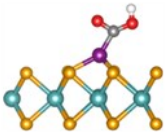	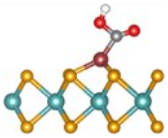	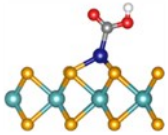	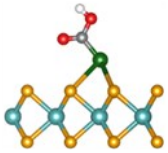	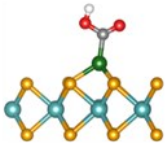

Fig. S5 Optimized structure of *COOH and *COOH' (initial structures are *OCHO) intermediates formed on $TM@MoSe_2$. The orange, blue, purple, brown, dark blue, green, grey, red and white balls represent Se, Mo, Fe, Co, Ni, Cu, C, O and H atoms, respectively.

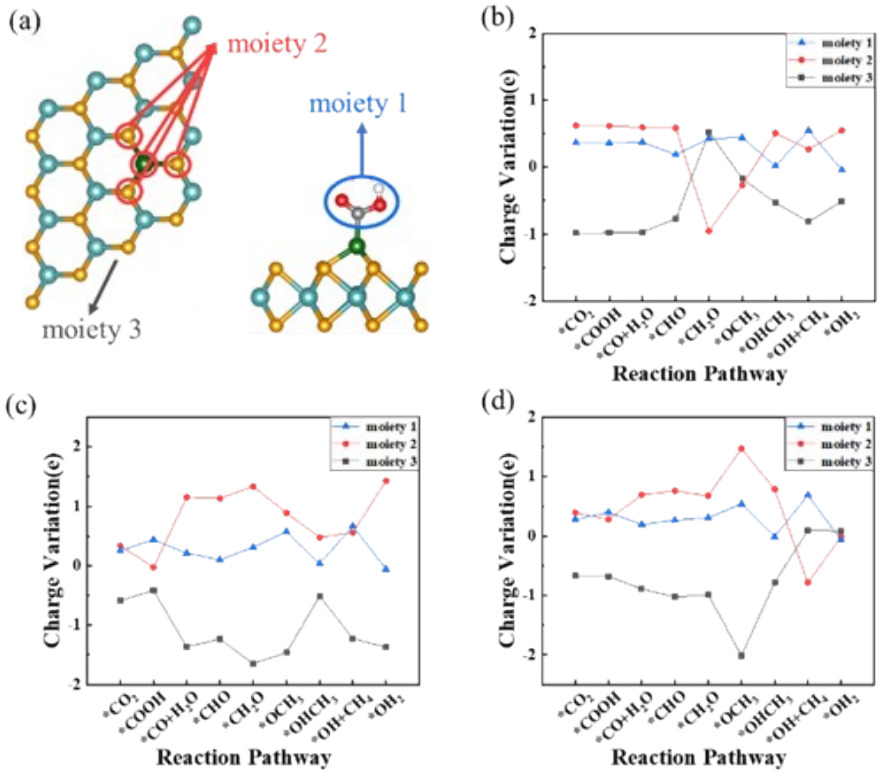

Fig. S6 (a) Top and side views of three moieties of the catalyst with *COOH intermediate. The orange, blue, green, grey, red and white balls represent Se, Mo, TM, C, O and H atoms, respectively. Charge variation of the three moieties along the reaction pathway on (b) Ni_{MT}@$MoSe_2$, (c) Cu_H@$MoSe_2$ and (d)Cu_{MT}@$MoSe_2$.

Table S1 Chemical potentials (μ) of gas-phase molecules obtained by summing up DFT electronic energy (E_{DFT}), zero point energy (ZPE), enthalpic temperature correction ($\int C_P dT$), and entropy contribution (–TS). [a] Data from Lim et al[1]. [b] Data from Peterson et al[2]. [c] Data from the current study. All data are given in eV.

Species	E_{DFT}[c]	ZPE[a](ZPEb)	$\int C_P dT$[b]	-TS[b]	μ(eV)
CH_4	-24.04	1.19(1.20)	0.10	-0.60	-23.34
CO_2	-22.95	0.28(0.31)	0.10	-0.65	-23.19
CO	-14.78	0.12(0.14)	0.09	-0.67	-15.22
CH_3OH	-30.22	(-1.35)	0.11	-0.79	-32.25
H_2	-6.77	0.3(0.27)	0.09	-0.42	-6.83
H_2O	-14.22	0.60(0.58)	0.10	-0.65	-14.19
HCOOH	-29.89	0.86(0.9)	0.11	-1.02	-29.90
CH_2O(HCHO)	-22.13	(-0.7)	0.10	-0.66	-23.39

Table S2 The electronic energy (E_{DFT}), zero point energy (ZPE), and entropy contribution (–TS) of adsorbate-surface systems. All data are given in eV.

Adsorbed species on Ni_{MT}@$MoSe_2$	**E_{DFT}**	**ZPE**	**-TS**
*COOH	-359.4365	0.5991	-0.1966
*CO	-349.7961	0.2013	-0.1011
*CHO	-352.0181	0.4336	-0.1501
*CH_2O	-355.7942	0.7099	-0.1532
*OCH_3	-359.6960	1.0581	-0.1350
*$OHCH_3$	-364.1471	1.4212	-0.2671
*OH	-343.4624	0.3227	-0.0896
*OH_2	-347.9677	0.6545	-0.1935
Adsorbed species on Cu_H@$MoSe_2$	**E_{DFT}**	**ZPE**	**-TS**
*COOH	-357.6122	0.5941	-0.1985
*CO	-346.4739	0.1645	-0.0981
*CHO	-349.9011	0.4396	-0.0948
*CH_2O	-353.4115	0.7508	-0.1459
*OCH_3	-358.0506	1.0672	- 0.2015
*$OHCH_3$	-361.5334	1.4113	-0.2754
*OH	-342.0096	0.3274	-0.1601
*OH_2	-345.3603	0.6349	-0.2170
Adsorbed species on Cu_{MT}@$MoSe_2$	**E_{DFT}**	**ZPE**	**-TS**
*COOH	-357.8521	0.5973	-0.1977
*CO	-346.5988	0.1848	-0.1191
*CHO	-350.1327	0.4435	-0.1519
*CH_2O	-352.8111	0.7655	-0.1713
*OCH_3	-358.1605	1.0727	-0.2328
*$OHCH_3$	-361.5658	1.4151	-0.2185
*OH	-342.0514	0.3222	-0.1044
*OH_2	-345.3997	0.6470	-0.1948

Table S3 The total energy of TM@$MoSe_2$ catalysts, binding energy (E_b, in eV) of the single transition metal atom in TM@$MoSe_2$. The data in parenthesis denote the cohesive energy of the transition metal in bulk.

Catalyst	Energy (eV)	Eb (eV)
Fe_H@$MoSe_2$	-333.24	-3.71
Fe_{ST}@$MoSe_2$	-331.74	-2.21
Fe_{MT}@$MoSe_2$	-333.64	-4.11
Co_H@$MoSe_2$	-332.97	-3.78
Co_{ST}@$MoSe_2$	-331.58	-2.39
Co_{MT}@$MoSe_2$	-333.33	-4.14
Ni_H@$MoSe_2$	-332.46	-3.52
Ni_{ST}@$MoSe_2$	-331.31	-2.37
Ni_{MT}@$MoSe_2$	-332.98	-4.04
Cu_H@$MoSe_2$	-330.56	-1.62
Cu_{ST}@$MoSe_2$	-330.56	-1.62
Cu_{MT}@$MoSe_2$	-330.64	-1.70

Table S4 The adsorption energy of H and CO_2 on TM@$MoSe_2$.

Catalyst	E_{ads}(H)	E_{ads}(CO_2)
Fe_{MT}@$MoSe_2$	-0.410	-0.886
Co_{MT}@$MoSe_2$	-0.090	-0.780
Ni_{MT}@$MoSe_2$	0.409	-0.405
Cu_H@$MoSe_2$	-0.308	-0.026
Cu_{MT}@$MoSe_2$	-0.589	-0.062

Table S5 The free energy change of the first protonation step of CO_2RR and HER.

Catalyst	ΔG(*COOH)	ΔG(*COOH')	ΔG(*H)
Fe_{MT}@$MoSe_2$	-0.021	0.007	-0.170
Co_{MT}@$MoSe_2$	0.173	0.444	0.150
Ni_{MT}@$MoSe_2$	0.639	0.639	0.649
Cu_H@$MoSe_2$	-0.304	-0.284	-0.068
Cu_{MT}@$MoSe_2$	-0.432	-0.432	-0.349

Table S6 The adsorption energy of CO, CH_2O, CH_3OH and CH_4 on TM@$MoSe_2$

Species	Ni_{MT}@$MoSe_2$	Cu_H@$MoSe_2$	Cu_{MT}@$MoSe_2$
$E_{ads}(CO)$	-2.230	-1.454	-1.427
$E_{ads}(CH_2O)$	-0.685	-0.720	-0.698
$E_{ads}(CH_3OH)$	-0.948	-0.752	-0.709
$E_{ads}(CH_4)$	-0.200	-0.198	-0.156

Table S7 Equilibrium potentials of several possible CO_2RR cathode reactions.

Cathode Reaction	$U_{equilibrium}$ vs RHE(V)
$CO_2+2H^++2e^-\rightarrow CO(g)+H_2O$	-0.11
$CO_2+2H^++2e^-\rightarrow HCOOH(l)$	-0.25
$CO_2+4H^++4e^-\rightarrow HCHO(l)+H_2O$	-0.07
$CO_2+6H^++6e^-\rightarrow CH_3OH(l)+H_2O$	0.02
$CO_2+8H^++8e^-\rightarrow CH_4(g)+2H_2O$	0.17

Table S8 DFT-predicted limiting potentials (U_L), overpotential (η) and potential determining steps (PDS) for the production of CH_4.

Catalyst	U_L vs RHE(V)	η(V)	PDS
Ru_3(Hexaiminotriphenylene)$_2$[3]	-0.71	0.91($U_{equilibrium}$=0.20 V)	*CO→*CHO
Graphene supported Ag SACs[4]	-0.56	0.73($U_{equilibrium}$=0.17 V)	*OH→*+H_2O
C_2N-graphene supported Ti SACs[5]	-0.50	0.67($U_{equilibrium}$=0.17 V)	*CO→*CHO
Boron nitride monolayer supported Mo SACs[6]	-0.45	/	*OH→*+H_2O
Cu(111)[7]	-0.97	/	*CO→*CHO
Cu_H@$MoSe_2$ (this work)	**-0.316**	**0.486($U_{equilibrium}$=0.17 V)**	***OH→*H_2O**

Table S9 Bader charge of the three moieties (the division into three moieties is illustrated in Figs 5a) in $Ni_{MT}@MoSe_2$, $Cu_H@MoSe_2$ and $Cu_{MT}@MoSe_2$.

Adsorbed species on $Ni_{MT}@MoSe_2$	**moiety 1 ($C_xH_yO_z$)**	**moiety 2 ($TMSe_3$)**	**moiety 3**
*CO_2	0.366	0.622	-0.988
*COOH	0.361	0.619	-0.981
*CO	0.373	0.597	-0.971
*CHO	0.187	0.585	-0.772
*CH_2O	0.428	-0.955	0.527
*OCH_3	0.441	-0.271	-0.17
*$OHCH_3$	0.019	0.511	-0.53
*OH	0.551	0.267	-0.818
*OH_2	-0.041	0.55	-0.508
Adsorbed species on $Cu_H@MoSe_2$	**moiety 1 ($C_xH_yO_z$)**	**moiety 2 ($TMSe_3$)**	**moiety 3**
*CO_2	0.255	0.337	-0.591
*COOH	0.438	-0.026	-0.412
*CO	0.212	1.153	-1.365
*CHO	0.101	1.133	-1.234
*CH_2O	0.312	1.335	-1.647
*OCH_3	0.572	0.89	-1.462
*$OHCH_3$	0.036	0.476	-0.512
*OH	0.666	0.56	-1.226
*OH_2	-0.057	1.429	-1.372
Adsorbed species on $Cu_{MT}@MoSe_2$	**moiety 1 ($C_xH_yO_z$)**	**moiety 2 ($TMSe_3$)**	**moiety 3**
*CO_2	0.28	0.393	-0.673
*COOH	0.399	0.279	-0.678
*CO	0.195	0.693	-0.888
*CHO	0.268	0.758	-1.026
*CH_2O	0.307	0.677	-0.985
*OCH_3	0.542	1.472	-2.014
*$OHCH_3$	-0.01	0.788	-0.778
*OH	0.69	-0.783	0.093
*OH_2	-0.068	-0.015	0.083

References

1. D. Lim, J. H. Jo, D. Y. Shin, J. Wilcox, H. C. Ham and S. W. Nam, *Nanoscale*, 2014, **6**, 5087-5092.
2. A. A. Peterson, F. Abildpedersen, F. Studt, J. Rossmeisl and J. K. Norskov, *Energy Environ. Sci.*, 2010, **3**, 1311-1315.
3. Y. Tian, Y. Wang, L. Yan, J. Zhao and Z. Su, *Appl. Surf. Sci.*, 2019, **467-468**, 98-103.
4. H. He and Y. Jagvaral, *Phys. Chem. Chem. Phys.*, 2017, **19**, 11436-11446.
5. X. Cui, W. An, X. Liu, H. Wang, Y. Men and J. Wang, *Nanoscale*, 2018, **10**, 15262-15272.
6. Q. Cui, G. Qin, W. Wang, L. Sun, A. Du and Q. Sun, *Beilstein J. Nanotechnol.*, 2019, **10**, 540-548.
7. D. Y. Shin, J. H. Jo, J.-Y. Lee and D.-H. Lim, *Comput. Theor. Chem.*, 2016, **1083**, 31-37.